SONIC: A Speed of Sound Measurement for Nanobubble Characterization

Jeas Grejoy Andrews[1], Sunaina[1], Tatek Temesgen[1], Peter Kusalik[1], Kelly Rees[2], Yihao Wang,[2] W. Russ Algar[2], Susana Y. Kimura[1,*]

[1] *Department of Chemistry, University of Calgary, Calgary, AB, Canada*

[2] *Department of Chemistry, University of British Columbia, Vancouver, BC, Canada*

*Corresponding author; Address: Department of Chemistry, University of Calgary, 2500 University Drive NW, Calgary, AB, T2N 1N4, Canada. Email: s.kimurahara@ucalgary.ca

Abstract

Nanobubbles (NBs)—gas inclusions in water with diameters < 1 μm—are of growing interest because of their unique properties and their potential for transformative applications. For example, it has been reported that NBs exist in water over long periods (*i.e.* weeks to months) and can act as free gas reservoirs. However, NBs are a source of scientific debate, particularly regarding characterization methods. Conventional methods, such as dynamic light scattering, nanoparticle tracking analysis, and nanoflow cytometry, cannot distinguish between nanoparticles and NBs since they are insensitive to the differences of the physical properties of the materials. However, acoustic (speed of sound) measurements can be used to quantify NBs because they rely on the compressibility dependence of gases (κ_{gas}) which is considerably larger than liquids (κ_{water}) and solids. In the present work, a speed of sound measurement for nanobubble characterization (SONIC) was designed and developed to probe the compressibility variations diagnostic to NBs in water. NBs in water act as acoustic scatters that reduce the speed of sound relative to the bubble-

free water. This decrease in the speed of sound can only be attributed to the existence of gas bubbles due to the strong compressibility dependence that solid nanoparticles lack. The results obtained from the acoustic measurements are compared with the observations from nanoparticle tracking analysis to confirm the existence of NBs in water. SONIC was validated in water with different molalities of NaCl (*aq*), and in the presence of solid nanoparticles of similar size and concentration to the NBs. SONIC is the first technique that addresses an important bottleneck of NB characterization by providing accurate and selective characterization of NBs in complex water mixtures that will help the behaviour of NBs to be better understood and accelerate their application in many fields.

Graphical Abstract

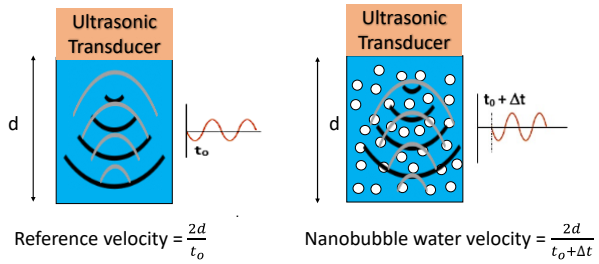

Keywords: Nanobubbles, Electric fields, Acoustic measurements, Nanoparticle tracking analysis, Ultrasound, Speed of Sound

Introduction

Bulk nanobubbles (NBs) are tiny gas inclusions suspended in liquids with a size less than 1 µm. NBs are increasingly being used in many applications including water treatment, medical imaging

and therapy, agriculture, aquaponics, algae control in surface waters, and algae growth for food. Diverse methods have been adopted to generate NBs in water, including electrolysis, solvent exchange, membrane methods, and cavitation methods such as hydrodynamic, ultrasonic, and electrostrictive cavitation.[1-7] NBs are reported to have lifetimes of days and weeks as opposed to the sub-ms timescales predicted by a classical lifetime analysis of the Epstein-Plesset and Young-Laplace equations.[8-11] This apparent contrast between the predicted and observed behaviors has resulted in much debate regarding their existence. The main challenge is the lack of NB-specific techniques to study their physical parameters, such as the density of the NB dispersion, net gas content inside the bubbles, true size, and population (NB concentration).

Due to difficulties in precisely identifying NBs, unambiguous confirmation of their existence has been impeded. Despite the availability of nanoparticle tracking analysis (NTA) and dynamic light scattering (DLS) to measure NB size, these measurements detect not only gaseous bubbles but also solid particles and liquid droplets, with no direct way to distinguish between these cases.[12-14] There have been several attempts to quantify NBs in water using a combination of physical and chemical methods. For example, the Winkler titrimetric method was used to evaluate the oxygen gas content in NB water that contained a NB volume fraction less than 10^{-7}.[15] However, the titrimetric method is not sensitive enough for a NB volume fraction less than 10^{-7}. In another study, the volume change for NBs in water after a degassing process was investigated but the results were inconclusive.[16]

Unlike DLS and NTA, speed of sound measurements can effectively differentiate NBs from nanoparticles because the density of a gas (ρ_{gas}) is significantly lower than the density of water (ρ_{water}) and solids, and the compressibility of a gas (κ_{gas}) is considerably larger than compressibility of water (κ_{water}) and solids.[17] For example, for an ideal gas at 20 ℃ and 1 atm, κ_{gas}

/κ_{water} is equal to 2.15 × 10^4. The speed of sound (c) at sufficiently low frequency in a fluid or fluid-fluid mixture is related to the density (ρ) and isentropic compressibility (κ):[18-20]

$$c = \frac{1}{\sqrt{\rho\kappa}} \quad (1)$$

When a bubble is present in a liquid, it has two distinct features: stiffness and inertia. The stiffness is due to the interface of the bubble that encloses a given volume of gas, which can be modeled to behave like a spring when disturbed. The inertial effects are due to the liquid region surrounding the bubble.[21, 22] These two features give rise to a natural frequency (f_0) for the bubble:

$$f_0 = \frac{1}{2\pi r}\sqrt{\frac{3p}{\rho_{water}}} \quad (2)$$

For instance, a NB radius (r) of 100 nm, a water density (ρ_{water}) of 998.20 kg/m^3, and an atmospheric pressure (p) of 88 kPa would result in a natural frequency of about 26 MHz. This result suggests that, for any transducer (a device that converts electrical signals into sound and *vice versa*) operating at a central frequency lower than 26 MHz, resonance effects will be avoided if there are no microbubbles present. Note that the speed of sound in the resonance range will be higher for NB water than for control water.[17]

The objective of this study is to develop a fast and reliable speed-of-sound measurement for NB characterization (SONIC) and compare it with NTA measurements. The key advantage of performing speed-of-sound measurements is that the acoustic properties are different for NB water versus ordinary water.[17, 18, 23] This feature helps to differentiate bubbles from solid components and quantify the total gas volume fraction within the NB water and thereby overcomes the limitations of current standard methods.

Experimental Section

Materials. High purity LC-MS Optima grade water with an ionic impurity of less than 20 μg/L from Fisher Scientific (Pittsburgh, USA) was used for NB generation. All glassware and the NB generator were cleaned with Extran 300 concentrate from EM Science (Gibbstown, USA), followed by ten rinses with deionized water and three rinses with 18.2 MΩ cm ultrapure water from a Thermo-Scientific Barnstead Smart2Pure UV Water Purification System (Massachusetts, USA). All other solutions were prepared with ultrapure water. Oxygen gas of 99.999% purity was purchased from Air Liquide (Quebec, Canada). Sodium chloride with a purity ≥ 99.0% from Sigma Aldrich (Missouri, USA) was used to make different concentrations in water to validate the method. Silica nanoparticles with an average diameter of 120 nm and a concentration of 10 mg/mL (Nanocomposix (California, USA)) were used to study the interference of nanoparticles with NBs on the speed-of-sound measurements.

Experimental setup for speed-of-sound measurements. The speed-of-sound was determined with the pulse-echo method using the instrumentation (Figure 1) that was developed in-house for this study. Custom-designed ultrasound transducers (0.5, 1, and 5 MHz) from Piezohannas (Hubei, China) were excited by a sine wave pulse of 4 cycles with a burst period of 10 ms and a peak-to-peak voltage of 10 V_{pp} using a Siglent 1032x Arbitrary waveform generator (Ohio, USA).

The excitation signal frequency was chosen to be the same as the transducer's central frequency. The designed electric burst excites the transducer and produces a sound wave pulse, which propagates through the acoustic cell and produces an echo after reaching the glass reflector of a known thickness. The initial electrical excitation and the response from the echo of the sound wave that passed through the acoustic cell were recorded with a sampling rate of 2 gigasamples/second

using a Siglent SDS 2102x Oscilloscope (Ohio, USA) having a maximum bandwidth of 100 MHz with a waveform averaging of 1024. Finally, the acoustic cell was maintained at a uniform temperature of 20 ℃ unless otherwise mentioned, with a thermal stability of ±0.1 ℃ using a VWR general-purpose thermal bath (Pennsylvania, USA). All temperature measurements were recorded with a calibrated VWR k-type thermocouple against a Polyscience calibration bath (Illinois, USA) of temperature stability ±0.005 ℃.

Acoustic Cell Design. Three acoustic cells were designed and built from borosilicate glass with various geometries, bottom thicknesses, and heights. The acoustic cells were tested to evaluate the design parameters that gave the best echo quality for the NB study. Two different geometries were chosen for the study and their schematics are shown in Figure 2. In the Type 'A' design (Fig. 2A,C), the diameter (D_1 = 2, 3, and 4 cm) was varied. In the Type 'B' design (Fig. 2B,D), flat glass plates of different thicknesses (X = 2, 5, 10, 50 mm) and lengths (L = 68.4 and 140.8 mm) were used with a D_2 = 3 cm.

Investigation of Salt Concentration, Temperature, and Frequency with SONIC. The speed of sound was evaluated using SONIC in ultrapure water and with NaCl mixtures at different molalities (0.0415, 0.0954, 0.1680, 0.3405, and 0.5041 m) at 25 °C. Experiments were conducted in triplicate. Temperature correction equations were developed as described in Text S1 of the supporting information (SI). The temperature of ultrapure water contained in the acoustic cell was controlled using a water bath (Illinois, USA) and a thermocouple. Temperatures were increased in 0.1 ℃ increments and equilibrated for 15 mins, and compared to a room-temperature control. Experiments were conducted in triplicate. Three frequencies (0.5, 1, and 5 MHz) were tested to verify the low-frequency transducer range required to measure NBs.

Nanobubble Generation. A lab-developed multistage generator that utilizes electric fields was used to generate bulk NBs.[8] The details and schematic of the NB generator are shown in Figure S3 in SI.

Nanobubble Characterization and Validation. Freeze-thaw experiments, dynamic light scattering (DLS) and nanoparticle tracking analysis (NTA)[24-27] were used for NB characterization. For the freeze-thaw experiments, NB samples were collected in two glass bottles. One bottle was frozen overnight in a VWR FFV-20 freezer (Pennsylvania, USA) at −10 ℃, and the other bottle was left at room temperature. The frozen water was melted and brought back to room temperature. Both bottles were tested using a red laser pointer to observe changes in the intensity of Tyndall scattering and were characterized by NTA. The control water (reference) consisted of water with 5 h of mixing with no electric field.

NB sizes were obtained with a DLS Zetasizer ZS (Malvern, UK). Sample (1 mL) was loaded in a cuvette (Sarstedt, Germany) made of polymethyl methacrylate. The experiment was performed at a scattering angle of 173° at a temperature of 20 °C. The refractive index of the gas and water was set to 1.00 and 1.33, respectively.[8] Measurements were done in triplicate. An NS300 NanoSight (Malvern Analytics, software version 3.3) was used to obtain NTA measurements for NB size and population. The measurements were conducted at room temperature using a blue laser light source with a wavelength of 488 nm. The sample was introduced using a syringe pump with a speed of ~10 μL/min. Three 30-second videos of diffusing NBs were recorded with a frame rate of 25 FPS using a high-speed sCMOS camera and NBs were tracked to obtain the population distribution of NBs in a given sample. A control water sample with no NBs, water with NBs, and a freeze-thawed sample originally containing NBs were analyzed for each sample set.

To confirm the specificity of the speed-of-sound measurements to NBs in the presence of solid inclusions, speed-of-sound measurements were conducted in a freshly prepared NB water sample (10^8 mL^{-1}) and spiked with SiO_2-NP to obtain a concentration of 5×10^8 SiO_2-NPs mL^{-1} in the final mixture. Measurements were conducted in triplicate.

The sensitivity of SONIC was evaluated with NB water samples that were drawn at different time intervals (T=0, 3, 6 hr) during NB generation that reflected increasing NB concentration with increasing NB generation time. NB water samples were also tested with NTA. From the NTA, the NB size and concentration data was converted to cumulative volume fraction by multiplying the NB population at each NB size by its corresponding volume. All the volume fractions for each NB size were added and compared with the volume fraction obtained by SONIC.

Results and Discussion

Acoustic Measurements. For a mixture containing gas in the form of bubbles in water, the volume fraction (ϕ) of bubbles in a given volume is represented as,

$$\phi = \frac{V_b}{V_b + V_w} \tag{3}$$

where V_b and V_w are the total gas bubble volume and water volume, respectively. In this case, the effective mixture density (ρ) and isoentropic compressibility (κ) are written as shown below:

$$\rho \approx \rho_{water}(1 - \phi) \tag{4}$$

$$\kappa = \kappa_{gas}\phi + \kappa_{water}(1 - \phi) \tag{5}$$

Combining Equations (4), (5), and (1) with some simplification ($\kappa_{water} \ll \kappa_{gas}, \phi^2$ is negligible, and $\kappa_{water}\phi$ is small) yields the speed of sound in the mixture (c_m):

$$\frac{1}{c_m^2} = \left(\rho_{water}\kappa_{water} + \rho_{water}\phi\kappa_{gas}\right) \quad (6)$$

From Eq (1), we define $\frac{1}{c_{ref}^2} = \rho_{water}\kappa_{water}$ that is substituted in Equation (6) to obtain,

$$\frac{1}{c_m^2} = \left(\frac{1}{c_{ref}^2} + \rho_{water}\phi\kappa_{gas}\right) \quad (7)$$

Equation (7) suggests that the speed of sound under low-frequency conditions in NB water would be lower compared to the reference water sample (c_{ref}). The measurement of the speed of sound is useful to quantitatively determine the total volume fraction of NBs present in a given volume of water. That is, the NB volume fraction can be determined from the time of flight, *t*, for sound through a sample over a constant and known distance. The speed of sound Equation (7) is similar to Equation 2(a) and the Wood's equation (6) in Temkin *et al.*[20] for low-frequencies speed of sound, as derived in detail in Text S2 in SI.

The speed of sound in water is sensitive to temperature such that the experimental quantification of NBs in the water would be affected by the temperature shifts that mask the effect of NBs. Therefore, any temperature variations need to be recorded and corrected. The data used for the temperature correction factor were obtained from the IAWPS-95 of Wagner and Pruß.[28] For an increase in temperature of 1 ℃, the speed of sound increases by a value of 3.0717 m/s over a linear fit of measured temperatures between 19 to 21℃. Therefore, if *T* is the departure from the reference temperature T_0, then the deviation in the speed of sound becomes,

$$c - c_o = 3.0717(T - T_0) \quad (8)$$

where c is the velocity at temperature T, and c_0 is the velocity at temperature T_0. Multiplying equation (8) by one (c_0/c_0), substituting $c = 2d/t$ and $c_0 = 2d/t_0$, and rearranging an expression is obtained for the corrected time of flight (t),

$$t = t_0 \left[1 + \frac{3.0717}{c_o}(T - T_o)\right]^{-1} \quad (9)$$

where, t_0 is the time of flight at the reference temperature (T_0). Equation (9) was used to correct for small fluctuations from the reference temperature, which is the setpoint in the thermal bath. When there are no fluctuations in the temperature, the time of flight at the reference temperature is the same as the corrected time of flight (t). The detailed derivation for equation (9) is shown in Text S1 of the SI.

For the reference temperature selected, the speed of sound in reference water (c_{ref}) is given by,

$$c_{ref} = \frac{2d}{t_{ref}} \quad (10)$$

where *d* is the actual depth of the acoustic cell in meters. The speed of sound in NB water mixture (c_m) was estimated using,

$$c_m = \frac{c_{ref} t_{ref}}{t_{ref} + \Delta t} - \frac{2d}{t_m} \quad (11)$$

where, t_m is the time of flight in the NB water mixture, Δt is the time shift in seconds between reference water and NB water obtained by computing the cross-correlation between the two time series, as described below. The value of c_{ref} was also obtained from Pruß and Wagner *et al.*[28]

Cross-correlation was used in this study to measure the similarity of two waveforms as time series as a function of the displacement of one relative to the other.[29] The cross-correlation, "$R_{xy}(\Delta t)$" of two real continuous functions, $x(t)$ and $y(t+\Delta t)$ is defined by,

$$R_{xy}(\Delta t) = \sum_t x(t)y(t+\Delta t) \tag{12}$$

When two correlated signals are compared, the function $R_{xy}(\Delta t)$ will be characterized by a maximum. The position of that maximum is useful for estimating the time difference (Δt) between the input functions x and y. A detailed explanation of the method is provided in Text S3 in the SI.

After determining the speed of sound in reference water (c_{ref}) and NB water mixture (c_m), the volume fraction of NBs in water is determined by rearranging equation (7) in the following manner:

$$\phi = \frac{1}{\rho_{water}\kappa_{gas}}\left[\frac{1}{c_m^2} - \frac{1}{c_{ref}^2}\right] \tag{13}$$

The isothermal compressibility of a fluid is given by,

$$\kappa = -\frac{1}{V}\left(\frac{dV}{dp}\right)_T \tag{14}$$

where V is the volume, and p is the pressure. Note that the V can be written in terms of Gibbs free energy under isothermal conditions as $\left(\frac{dG}{dp}\right)_T$, and use of this relation in equation 14 enables identification of κV with the second derivative of G. This second derivative function makes the speed of sound more sensitive to the existence of NBs in water compared to the first derivative. Assuming the sample is at 20 ℃ and 0.88 bar (average value of atmospheric pressure in Calgary, Canada) and that the gas behaves ideally, the isothermal compressibility of oxygen is given by,

$$\kappa_{gas} = \frac{1}{P} = 11.36 \times 10^{-6}\ Pa^{-1} \quad (15)$$

Similarly, the density of water at 20 ℃ and 0.88 bar from IAPWS-95 was found to be 998.1963 kg/m^3.[28] Substituting the density of water (ρ_{water}), the compressibility of oxygen (κ_{gas}), equations 10 and 11 into equation 13 and with rearranging yields,

$$\phi = \frac{88.20}{(c_{ref} t_{ref})^2}\left[t_m^2 - t_{ref}^2\right] \quad (16)$$

Finally, the number of NBs in a sample volume is determined by incorporating the mean size of NBs obtained from DLS or NTA measurements. The number of NBs in 1 mL of the sample, *n*, can then be determined from,

$$n = \frac{\phi}{v_b} \quad (17)$$

where v_b is the volume of a single NB in units of mL.

Optimization of the Acoustic Cell. An optimized acoustic cell is essential for the speed-of-sound measurements to be sensitive enough for NB quantification. The electrical response collected by the oscilloscope requires a clear signal that is free from unwanted noise, such as those produced from cell wall surfaces. Recorded echoes typically had three regions: the desired response from the glass reflector, the unwanted interactions with the cell wall surface, and other indirect sources.[30] Therefore, we aimed to minimize unwanted reflections of the acoustic pulse that would result in erroneous cross-correlation and time delays.

First, the Type "A" design with different diameters (2, 3, and 4 cm) were tested for echo quality and are shown in Figure S4 in the SI. The echoes in all three cells were severely affected by

additional signals. The echo from the 2 cm internal diameter cell (Figure S4A in SI) has a moderate amplitude but also had unwanted reflections, both before and after the main signal. Similarly, the reflections from the target and other surfaces were not easily distinguished. For cells with diameters of 3 and 4 cm (Figure S4B and S4C in the SI), the surface reflections were reduced; however, the echoes did not have well-defined shapes and the main signal was attenuated, which might be attributed to either the mounting of the transducer or to the irregularities on the cell bottom. These two aspects were considered for the Type "B" design. Additionally, a 3 cm diameter cell was used because it was the only size available that we can perform additional modifications for further testing.

For the Type "B" design, the glass cell had an internal diameter of 3 cm, a wall thickness of 2.5 mm, length of 68.39 mm and the cell bottom/glass reflector was fitted with a flat smooth glass plate of different thicknesses (2, 5, 10, and 50 mm). A longer cell length of 140.83 cm with a glass reflector of 50 mm was also tested to evaluate if the cell length affected the echo quality. The top of the acoustic cell was fitted with a glass flange to connect firmly with the transducer to maintain a constant distance in experiments for reproducibility. As shown in Figure 3, the main echo from the reflector with 2 mm thickness (Figure 3A) was slightly distorted from the general wavelet shape, where only the start of the echo was reasonably apparent and the exact echo position could not be determined. The response from the reflector with 5 mm and 10 mm thickness had similar signals (Figures 3B and 3C) that were somewhat improved; however, these echoes still overlapped with the signals from side reflections such that the end of the echo region was not easily distinguishable. The reflector with 50 mm thickness (Figure 3D) provided a distinct improvement in the signal-to-noise ratio and both the start and end of the main echo were well defined. The optimum thickness for the reflector for the pulse-echo arrangement was therefore chosen to be 50

mm. A cell with a longer length (L = 140.83 mm) was also tested (Figure 3E) and the echo was similar to Figure 3D (L = 68.39 mm), suggesting that cylinder length did not affect the quality of the signal. For this reason, and because it required smaller sample volumes, the shorter cell was selected. The path length of the shorter cell—twice the L—was calibrated experimentally to be 136.788 ± 0.005 mm as explained in Text S4 in the SI.

Effects of Salinity, Temperature, and Frequency. The velocity shifts with increasing salt concentration in water were measured to validate that SONIC accurately measures the speed of sound. The data, shown in Figure 4, were fitted by linear regression with a coefficient of determination (R^2) value > 0.999, agreed with values reported in literature,[31,32] and had an uncertainty of $\pm$0.02 m/s or better.

To confirm the accuracy of the temperature correction via equation 9, experiments were conducted at different temperatures and compared to control experiments at 20.1 ℃ (see Table S2 in the SI). Results indicate that the corrected time of flight yielded 92.270 μs which deviates slightly from the reference temperature 92.265 μs by 0.005 μs. These results validate the temperature correction via equation 9.

Three frequencies (0.5, 1, and 5 MHz) were tested to verify the low-frequency transducer range required to measure NBs. For this analysis, NB water samples were prepared and evaluated with SONIC. As shown in Figure 5, the three measured speed of sound were statistically the same and therefore, the transducer's frequency did not significantly affect the measured speed of sound in NB water. In addition, since none of the velocities measured with 0.5, 1, and 5 MHz transducers exceeds the speed of sound for pure water, the effect of resonance was not apparent in the analysis.

These results also confirmed that there were no microbubbles (≥1μm) present (which would be expected to resonate at these frequencies) in the measured NB water sample. The negligible variations observed in the values for speed of sound may have arisen from inconsistency in the placement of the active element inside the transducer casing or acoustic impedance mismatch of the transducer casing.

Nanobubbles measurement and validation. After NB generation, NB water samples were visually inspected with a red laser and freeze-thaw experiments. Images of the pure water, NB water, and freeze-thawed NB water are shown in Figure S5 in SI. The NB water had a bright optical path from light scattering by NBs whereas the freeze-thawed NB water did not exhibit strong scattering. Furthermore, the scattering intensity for the freeze-thawed water and the reference water were similar, which suggested that NBs were removed during the freezing and thawing process. Cryo-scanning electron microscopy images were also obtained for NB water and reference water (Figure S10 in the SI) and discussed in Text S4 in the SI.

Speed-of-sound measurements were performed by recording the time-of-flight in freshly prepared NB water samples and compared with the ultrapure water sample. These measurements were used to quantify the total NB volume fraction in solution with equation 16. Results are shown in Figure 6. The time-of-flight of the ultrasound waves in NB water was 92.610 ± 0.034 μs, which was higher than the control sample at 92.270 ± 0.003 μs. The time-of-flight is longer in NB water due to the higher total compressibility of the sample, which translated into a 0.4% decrease of the speed of sound from 1482.6 ± 0.4 to 1477.0 ± 0.55 m/s. The NB volume fraction was calculated to be

$3.0\ (\pm\ 0.3) \times 10^{-7}$. The NB mean size of 150 nm from DLS measurements was used to obtain the average NB concentration of $1.7\ (\pm\ 0.2) \times 10^{8}$ NBs per mL.

The NB population obtained from SONIC was compared to values obtained by the NTA. The NTA software detects and monitors individual nanoscale entities in motion due to Brownian forces and correlates this motion with size using the Stokes-Einstein equation.[33] NTA can also count individual tracked particles, a direct measurement of particle concentration. Example video frames obtained for the reference water, NB water, and freeze-thawed NW water are shown in Figures S6-S8 in the SI. The video frames of the reference water and freeze-thawed water had 0.9 ± 0.2 particle counts per frame, significantly lower than the NB water with a value of 10.5 ± 0.4 suggesting that the entities being counted are NBs. The NB water had an average volume fraction of $2.27\ (\pm\ 0.09) \times 10^{-7}$, representing a cumulative nanobubble concentration of $1.23\ (\pm\ 0.09) \times 10^{8}$ NBs per mL (Figure S9 in SI). These results are similar to those obtained by SONIC. The reference water and freeze-thawed water had NB population distributions below or near to the detection limit of the instrument.[26]

Sensitivity of SONIC. The sensitivity of SONIC was evaluated by measuring the speed of sound in water with varying NB populations, reported as NB volume fraction. The NB generator was run for 1 and 3 h. Increasing generation time produced higher NB populations. Measurements were systematically compared with NTA, as shown in Figure 7. The volume fraction of NBs increased from $6.96\ (\pm\ 3.08) \times 10^{-9}$ at 1 h to $4.29\ (\pm\ 8.2) \times 10^{-8}$ at 3 h. The NB water sample at 3 h was subjected to freeze-thaw process and the speed of sound difference from the ultrapure water was negligible. According to the NTA, the NB population that was measured with SONIC at 1 h was

2.79 (± 0.19) × 10^7 per mL with mean size of 74.9 (± 3.1) nm and at 3 h was 5.30 (± 0.64) × 10^7 per mL with mean size of 77.5 (± 2.6) nm.

Nanobubble measurement in presence of solid particles. Experiments were conducted to evaluate the effect of solid particles on the speed of sound measurements in NB water. As shown in Figure 8, the presence of solid nanoparticles did not significantly affect the measurements, with consistent values recorded for a NB sample and a NB + SiO_2-NP sample. This result confirms that SONIC is sensitive to NB in water but insensitive to solid particles within the same solution.

Conclusion

SONIC is an ultrasound-based method for the characterization of NBs. Two acoustic cell designs were built and tested. Initial testing of design "A" found that an internal diameter of 3 cm produced a good signal and was incorporated in an optimized design "B," which had the transducer placed flush on the top of the cell with a 5 cm thick bottom glass plate. This configuration resulted in well-defined boundaries for the main echo signal for speed-of-sound measurements. The final acoustic cell design was validated by measuring the speed of sound with water with different molalities of salt. The effects of frequency and temperature variations were also evaluated. Then, SONIC was used to measure the volume fraction of NBs and compared to standard techniques. The average NB population obtained by SONIC was similar to the value obtained by NTA. Unlike other methods, SONIC is sensitive and selective to NBs and not prone to measurement artifacts from solid particles in samples. It is thus a highly promising method for analyzing NBs in complex

mixtures that can further advance the application of NBs in water treatment, health, energy and food industries.

Conflict of interest

The authors declare NO competing (financial or non-financial) interests, or other conflicts of any kind.

Supporting Information: Additional text is included that provides in detail the development of equations, the cross-correlation method, and the calibration of the acoustic cell; figures that depict a schematic of the nanobubble generator, results from Type "A" design, results of the Tyndall effect of nanobubble samples and controls, video frames of NB water samples and controls from NTA measurements; NTA size distribution data; and a table with time-of-flight measurements at different temperatures.

Acknowledgments

The authors want to thank the following University of Calgary staff and students: Mark Toonen, for his incredible help and creativity in creating the acoustic cell; Tood D. Willis, Nik Hamilton, Richard Galambos, Jaden Sprong, and Duncan Hanna, for their tremendous help in constructing the nanobubble generator and accessories; Stan Pankratz, Jianwei Chen, and Richard Adamson for the insightful discussions and advice that helped start this project; Drs. Matt Vijayan and Jithne Jayakumar Rajeswri for the training and use of their NTA equipment. Funding was provided by the Natural Sciences and Engineering Research Council (NSERC) Discovery Grant, NSERC

Alliance Grant, the NSERC Alliance-Alberta Innovates Advance Program, Canada Research Chair, and Canada Foundation for Innovation.

References

1. Postnikov, A. V.; Uvarov, I. V.; Lokhanin, M. V.; Svetovoy, V. B., Electrically controlled cloud of bulk nanobubbles in water solutions. *PLOS ONE* **2017,** *12* (7), e0181727.

2. Li, T.; Cui, Z.; Sun, J.; Jiang, C.; Li, G., Generation of Bulk Nanobubbles by Self-Developed Venturi-Type Circulation Hydrodynamic Cavitation Device. *Langmuir* **2021,** *37* (44), 12952-12960.

3. Wu, M.; Yuan, S.; Song, H.; Li, X., Micro-nano bubbles production using a swirling-type venturi bubble generator. *Chem. Eng. Process.* **2022,** *170*, 108697.

4. Wiraputra, I. G. P. A. E.; Edikresnha, D.; Munir, M. M.; Khairurrijal, Generation of Submicron Bubbles using Venturi Tube Method. *J. Phys. Conf. Ser.* **2016,** *739*, 012058.

5. Peng, F. F.; Yu, X., Pico–nano bubble column flotation using static mixer-venturi tube for Pittsburgh No. 8 coal seam. *Int. J. Min. Sci. Technol.* **2015,** *25* (3), 347-354.

6. Yasuda, K.; Matsushima, H.; Asakura, Y., Generation and reduction of bulk nanobubbles by ultrasonic irradiation. *Chem. Eng. Sci.* **2019,** *195*, 455-461.

7. Mo, C.-R.; Wang, J.; Fang, Z.; Zhou, L.-M.; Zhang, L.-J.; Hu, J., Formation and stability of ultrasonic generated bulk nanobubbles. *Chinese Phys. B* **2018,** *27* (11), 118104.

8. Ghaani, M. R.; Kusalik, P. G.; English, N. J., Massive generation of metastable bulk nanobubbles in water by external electric fields. *Sci. Adv.* **2020,** *6* (14), eaaz0094.

9. Zhang, X. H.; Khan, A.; Ducker, W. A., A Nanoscale Gas State. *Phys. Rev. Lett.* **2007,** *98* (13), 136101.

10. Fang, Z.; Wang, L.; Wang, X.; Zhou, L.; Wang, S.; Zou, Z.; Tai, R.; Zhang, L.; Hu, J., Formation and Stability of Surface/Bulk Nanobubbles Produced by Decompression at Lower Gas Concentration. *J. Phys. Chem. C* **2018,** *122* (39), 22418-22423.

11. Epstein, P. S.; Plesset, M. S., On the stability of gas bubbles in liquid-gas solutions. *J. Chem. Phys.* **1950,** *18* (11), 1505-1509.

12. Eklund, F.; Alheshibri, M.; Swenson, J., Differentiating bulk nanobubbles from nanodroplets and nanoparticles. *Curr. Opin. Colloid Interface Sci.* **2021,** *53*, 101427.

13. Zhou, L.; Wang, S.; Zhang, L.; Hu, J., Generation and stability of bulk nanobubbles: A review and perspective. *Curr. Opin. Colloid Interface Sci.* **2021,** *53*, 101439.

14. Hassan, P. A.; Rana, S.; Verma, G., Making Sense of Brownian Motion: Colloid Characterization by Dynamic Light Scattering. *Langmuir* **2015,** *31* (1), 3-12.

15. Kikuchi, K.; Ioka, A.; Oku, T.; Tanaka, Y.; Saihara, Y.; Ogumi, Z., Concentration determination of oxygen nanobubbles in electrolyzed water. *J. Colloid Interface Sci.* **2009,** *329* (2), 306-309.

16. Kim, E.; Choe, J. K.; Kim, B. H.; Kim, J.; Park, J.; Choi, Y., Unraveling the mystery of ultrafine bubbles: Establishment of thermodynamic equilibrium for sub-micron bubbles and its implications. *J. Colloid Interface Sci.* **2020,** *570*, 173-181.

17. Leroy, V.; Norisuye, T., Investigating the Existence of Bulk Nanobubbles with Ultrasound. *Chemphyschem* **2016,** *17* (18), 2787-90.

18. Wilson, P. S.; Roy, R. A., An audible demonstration of the speed of sound in bubbly liquids. *Am. J. Phys.* **2008,** *76* (10), 975-981.

19. Lamarre, E.; Melville, W. K., Instrumentation for the Measurement of Sound Speed near the Ocean Surface. *J. Atmos. Ocean. Technol.* **1995,** *12* (2), 317-329.

20. Temkin, S., Attenuation and dispersion of sound in dilute suspensions of spherical particles. *J. Acoust. Soc. Am.* **2000,** *108* (1), 126-146.

21. Medwin, H., Counting bubbles acoustically: a review. *Ultrasonics* **1977,** *15* (1), 7-13.

22. Chen, X.; Hussein, M.; Becker, T., Determination of bubble size distribution in gas-liquid two-phase systems via an ultrasound-based method. *Eng. Life Sci.* **2017,** *17* (6), 653-663.

23. Gibson, F. W., Measurement of the Effect of Air Bubbles on the Speed of Sound in Water. *J. Acoust. Soc. Am.* **1970,** *48* (5B), 1195-1197.

24. Aya, N.; Iki, N.; Shimura, T.; Shirai, T.; Kobayashi, H.; Maeda, S.; Kashiwa, M.; Fujita, T., Measurements of ultrafine bubbles using different types of particle size measuring instruments. In *International Conference on Optical Particle Characterization (OPC 2014)*, 2014.

25. Wu, C.; Nesset, K.; Masliyah, J.; Xu, Z., Generation and characterization of submicron size bubbles. *Adv. Colloid Interface Sci.* **2012,** *179-182*, 123-32.

26. Oh, S. H.; Kim, J. M., Generation and Stability of Bulk Nanobubbles. *Langmuir* **2017,** *33* (15), 3818-3823.

27. Ke, S.; Xiao, W.; Quan, N.; Dong, Y.; Zhang, L.; Hu, J., Formation and Stability of Bulk Nanobubbles in Different Solutions. *Langmuir* **2019,** *35* (15), 5250-5256.

28. Wagner, W.; Pruß, A., The IAPWS Formulation 1995 for the Thermodynamic Properties of Ordinary Water Substance for General and Scientific Use. *J.Phys. Chem. Ref. Data* **2002,** *31* (2), 387-535.

29. Cents, A. H. G.; Brilman, D. W. F.; Versteeg, G. F.; Wijnstra, P. J.; Regtien, P. P. L., Measuring bubble, drop and particle sizes in multiphase systems with ultrasound. *AIChE Journal* **2004,** *50* (11), 2750-2762.

30. Wilson, P., Sound propagation and scattering in bubbly liquids. Doctor of Philosophy, Boston University, Boston, MA. **2002**.

31. Chen, C.-T. A.; Chen, L.-S.; Millero, F., Speed of sound in NaCl, $MgCl_2$, Na_2SO_4, and $MgSO_4$ aqueous solutions as functions of concentration, temperature, and pressure. *J. Acoust. Soc. Am* **1978,** *63*, 1795-1800.

32. Sakurai, M.; Nakajima, T.; Komatsu, T.; Nakagawa, T., Apparent Molal Compressibility of Sodium Chloride in Water. *Chem. Lett.* **1975,** *4* (9), 971-976.

33. Nirmalkar, N.; Pacek, A. W.; Barigou, M., On the Existence and Stability of Bulk Nanobubbles. *Langmuir* **2018,** *34* (37), 10964-10973.

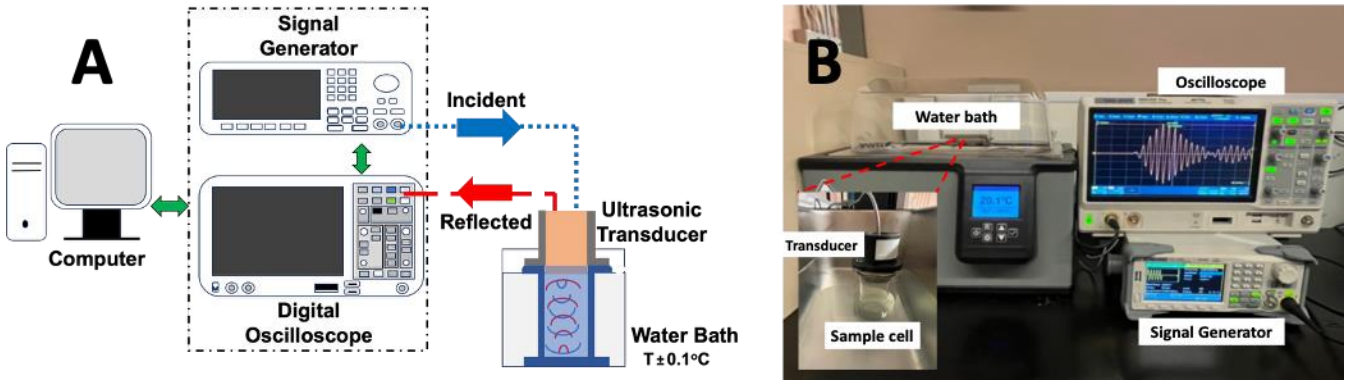

Figure 1: SONIC's schematic (A) and experimental setup (B).

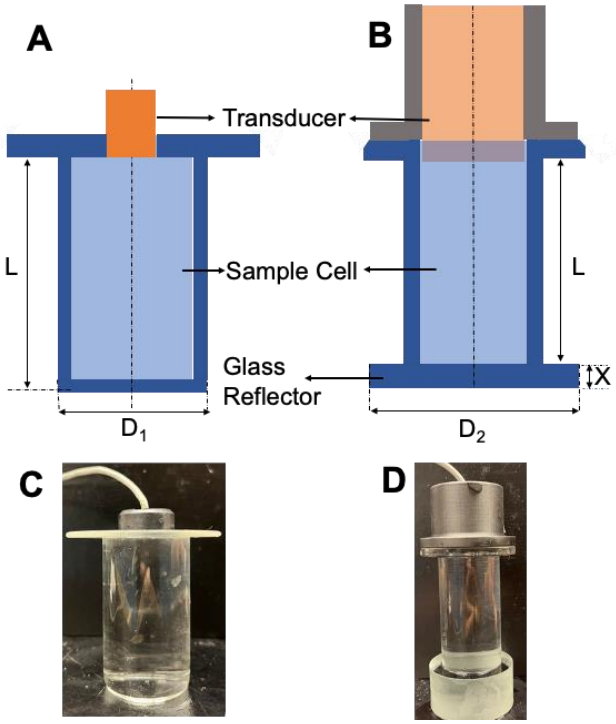

Figure 2: Schematic for the acoustic cells designed for the acoustic measurements A) Type "A" design D_1= 3 cm, L~ 68 mm and B) Type "B" design with D_2= 3 cm, and X = 50 mm, L=68.39 mm. Actual acoustic cell for C) Type "A" and D) Type "B".

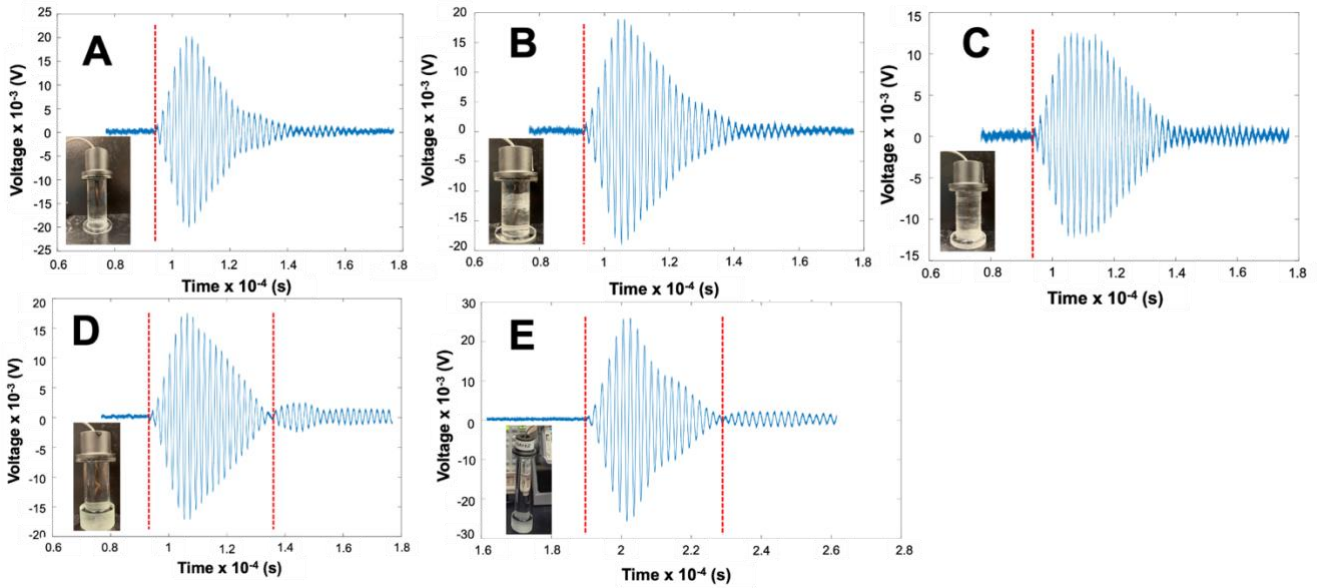

Figure 3: The transducer signal (in volts) and echo waveforms recorded by the oscilloscope for the type 'B' design of the acoustic cell with glass reflector thicknesses of 2 mm (A), 5 mm (B), 10 mm (C), 50 mm (D) all for a cell length of 68.39 mm, and 50 mm (E) for a cell length of 140.83 mm. All waveforms were recorded with an acoustic cell loaded with pure water. The red lines mark the start (A–E) and end (D&E) of the echo waveforms, delimiting the main signal. The photograph in each panel shows the acoustic cell that was tested.

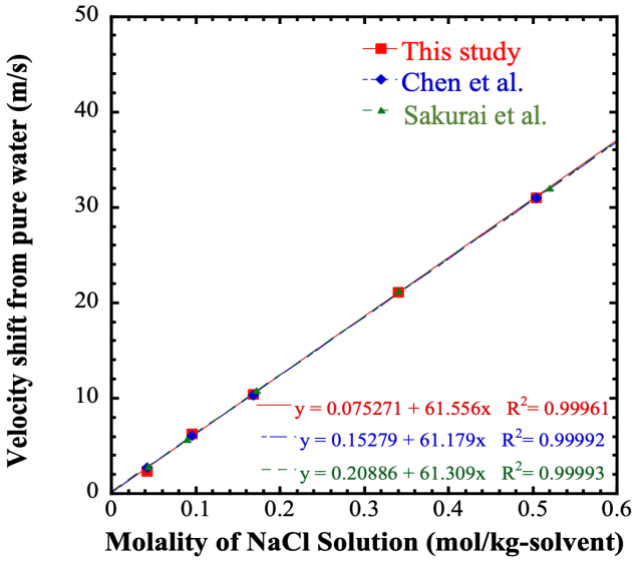

Figure 4: Variation of the speed of sound in NaCl (*aq*) solutions of different molalities and comparison with previously reported values.[31,32] A 5 MHz pulse-echo transducer was used for the experiments.

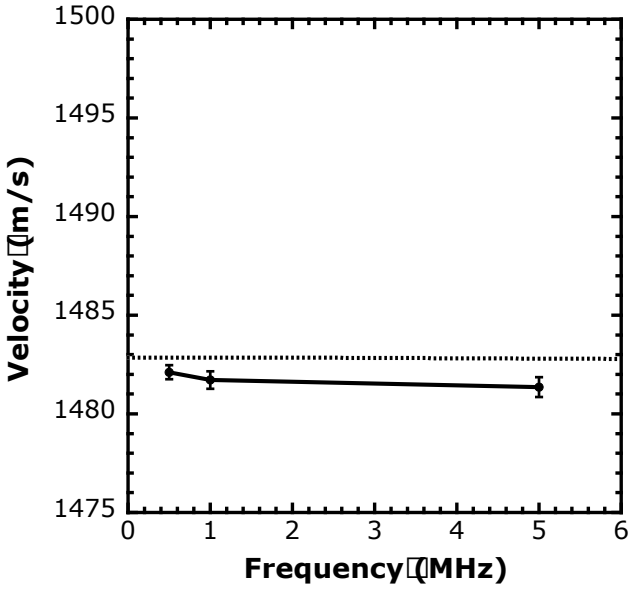

Figure 5: Effect of transducer frequency on the measured speed of sound in NB water. The dotted line corresponds to the value for pure water.

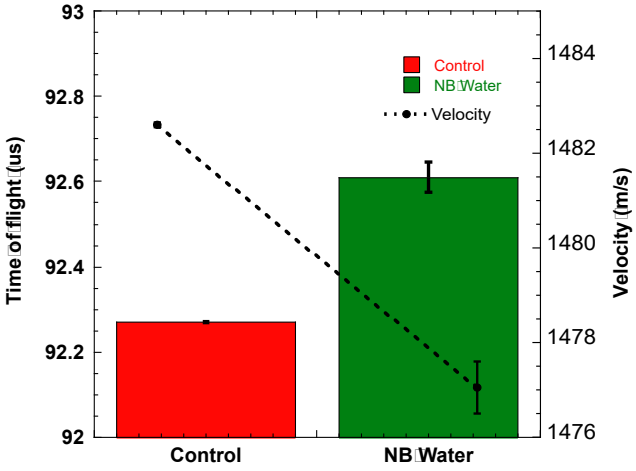

Figure 6: Measured time-of-flight (colored bars) and velocity in control (*i.e.* pure water) and NB water (black data points)

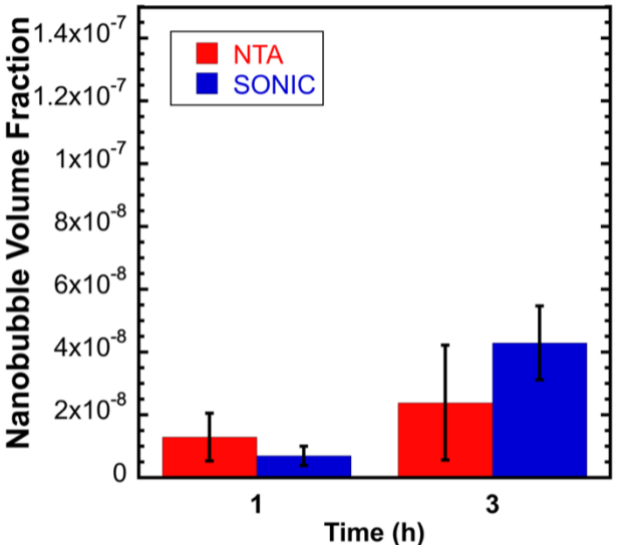

Figure 7: Comparison of nanobubble samples measured by NTA and SONIC.

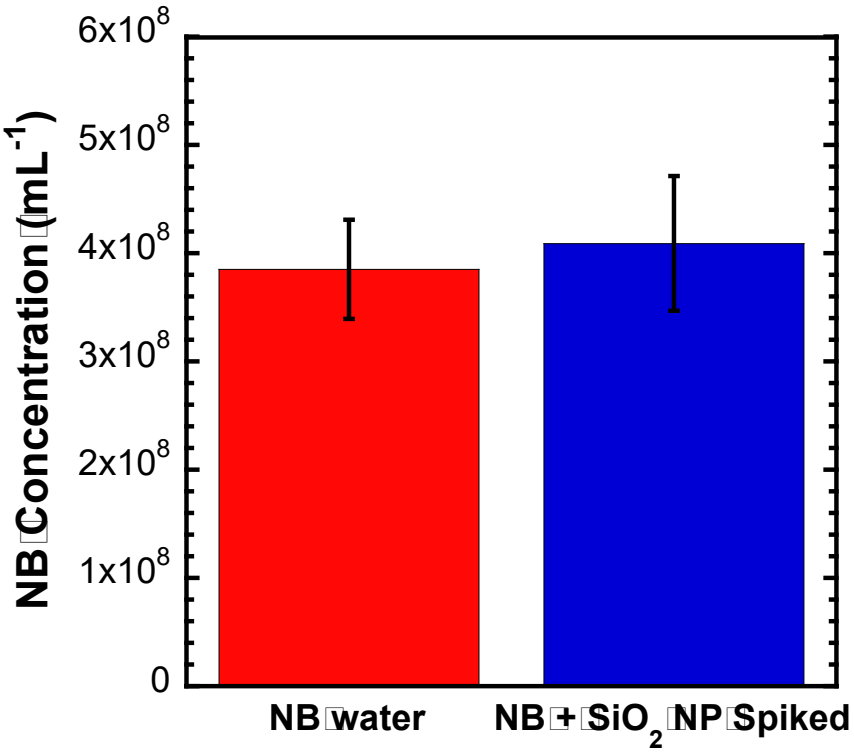

Figure 8: Comparison of the NB concentration (per mL) measured by SONIC for NB water and NB water spiked with SiO_2-NPs at a concentration of 5×10^8 NPs/mL.